AD-A140 924 FUNDAMENTAL STUDIES OF GROWTH DOPING AND TRANSFORMATION IN BETA SILICON C..(U) NORTH CAROLINA STATE UNIV RALEIGH SCHOOL OF ENGINEERING R F DAVIS ET AL. 1/1

UNCLASSIFIED 15 MAR 84 NCSU-243-043-004 N00014-79-C-0121 F/G 7/2 NL

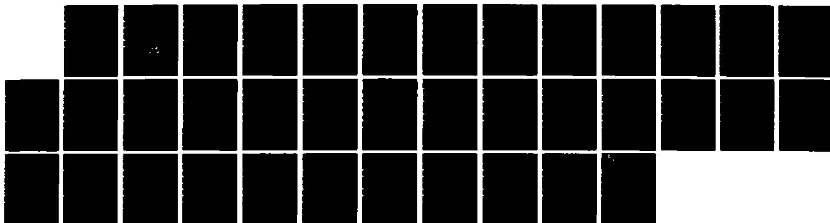

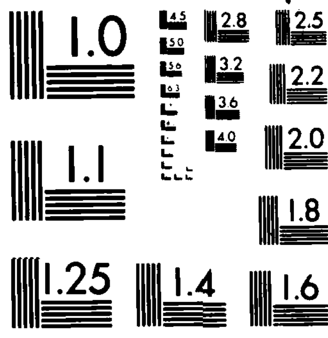

MICROCOPY RESOLUTION TEST CHART
NATIONAL BUREAU OF STANDARDS 1963 A

AD-A140 924

Annual Letter Report

FUNDAMENTAL STUDIES OF GROWTH, DOPING AND TRANSFORMATION IN BETA SILICON CARBIDE

Supported by ONR under Contract N00014-82-K-0182

March 1984

Report #243-043-004

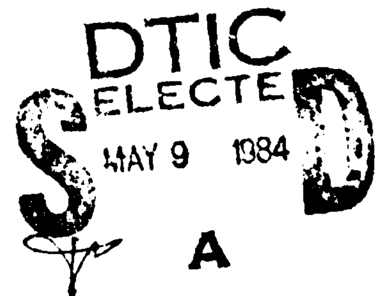

DTIC FILE COPY

School of Engineering
North Carolina State University
Raleigh, North Carolina

(14)

Annual Letter Report

FUNDAMENTAL STUDIES OF GROWTH, DOPING AND TRANSFORMATION IN BETA SILICON CARBIDE

Supported by ONR under Contract N00014-82-K-0182

March 1984

Report #243-043-004

DTIC
ELECTE
MAY 3 1984

SECURITY CLASSIFICATION OF THIS PAGE (When Data Entered)

REPORT DOCUMENTATION PAGE

READ INSTRUCTIONS BEFORE COMPLETING FORM

1. REPORT NUMBER: 243-043-004
2. GOVT ACCESSION NO.: AD-A140924
3. RECIPIENT'S CATALOG NUMBER:
4. TITLE (and Subtitle): Fundamental Studies of Growth, Doping and Transformation in Beta Silicon Carbide
5. TYPE OF REPORT & PERIOD COVERED: Annual Letter Report
6. PERFORMING ORG. REPORT NUMBER:
7. AUTHOR(s): Robert F. Davis, H. H. Stadelmaier
8. CONTRACT OR GRANT NUMBER(s): N00014-79-C-0121
9. PERFORMING ORGANIZATION NAME AND ADDRESS:
10. PROGRAM ELEMENT, PROJECT, TASK AREA & WORK UNIT NUMBERS: PE 61153N, RR 021-02-03, NR 243-027
11. CONTROLLING OFFICE NAME AND ADDRESS: ONR-427, Arlington, VA 22217
12. REPORT DATE: March 15, 1984
13. NUMBER OF PAGES: 32
14. MONITORING AGENCY NAME & ADDRESS (if different from Controlling Office): North Carolina State University, Department of Materials Engineering, 229 Riddick Laboratories, Raleigh, N. C. 27695-7907
15. SECURITY CLASS. (of this report): Unclassified
15a. DECLASSIFICATION/DOWNGRADING SCHEDULE:
16. DISTRIBUTION STATEMENT (of this Report): Approved for public release; distribution unlimited
17. DISTRIBUTION STATEMENT (of the abstract entered in Block 20, if different from Report):
18. SUPPLEMENTARY NOTES: ONR Scientific Officer; Tel: (202) 696-4218
19. KEY WORDS (Continue on reverse side if necessary and identify by block number):

Silicon Carbide	"in situ" doping	r-f sputtering
Crystal Growth	Annealing	Plasma Etching
Vapor Phase Epitaxy	Ion Microanalysis	Device Preparation
Ion Implantation	Oxidation	Electrical Properties

20. ABSTRACT (Continue on reverse side if necessary and identify by block number)

Electronic quality β-SiC thin films grown by CVD on Si substrates have been implanted with B^+, Al^+, P^+ and N^+ ions or doped with B^+ and Al^+ during growth. Rapid thermal annealing or resistive heating of the implanted samples up to 1653K for five minutes cause only modest activation of the charge carriers. Oxidation, plasma etching, electrical characterization and preparation for device fabrication have also been conducted.

DD FORM 1 JAN 73 1473 EDITION OF 1 NOV 65 IS OBSOLETE
S/N 0102-014-6601

Enclosure (1)

SECURITY CLASSIFICATION OF THIS PAGE (When Data Entered)

TABLE OF CONTENTS

		Page
I.	Introduction	1
II.	Doping of the β-SiC Thin Films During Growth	3
III.	Ion Implantation and Annealing Studies	19
IV.	Oxidation Studies	24
V.	Plasma Etching and RF Sputtering Research	27
VI.	Device Fabrication and Electrical Characterization	28

Dist
A-1

I. INTRODUCTION

Silicon carbide is the only compound species that exists in the solid state in the Si-C system and can occur in the cubic (C), hexagonal (H) or rhombohedral (R) structures. It is also classified as existing in the beta and alpha modifications. The beta, or cubic, form crystallizes in the zincblende or sphalerite structure; whereas, a large number (approximately 140) of the alpha occur in the hexagonal or rhombohedral forms known as polytypes.

Because of the emerging need for high temperature, high frequency and high power electric devices, blue L.E.D.'s, Schottky diodes, U. V. radiation detectors, high temperature photocells and heterojunction devices, silicon carbide is being examined throughout the world for employment as a candidate material in these specialized applications. The electron Hall mobility of high purity undoped β-SiC has been postulated from theoretical calculations to be greater than that of the α-forms over the temperature range of 300-1000K because of the smaller amount of phonon scattering in the cubic material. The energy gap is also less in the β-form (2.3 eV) compared to the α-forms (e.g., 6H = 2.86 eV). Thus, the β-form is now considered more desirable for electronic device applications, and, therefore, improvements in the growth and the characterization of thin films of this material constitute principal and ongoing objectives of this research program.

Under the previous grant, a method for the growth of single crystal thin films of β-SiC on (100) Si was developed using specially designed and very closely controlled variable pressure equipment and a two-step process. This method entails the initial chemical conversion of the Si surface via a high temperature reaction with ethylene (C_2H_4). This step is followed by direct and continual deposition of β-SiC via the separate decomposition of SiH_4 and C_2H_4 on the converted layer. H_2 is the carrier gas in both processes. Additional related research thrusts which have been conducted since that time include computer assisted calculations of CVD phase diagrams in the Si-C system, investigation of the physicochemical nature of the

converted layer, ion implantation and annealing studies, electrical measurements and development of simple devices.

The specific topics addressed in this reporting period include "in-situ" doping of the films during growth, continuation of the ion implant annealing program, oxidation of the β-SiC films and continued work on device development. All of these topics are described in the succeeding sections.

II. DOPING OF THE β-SiC THIN FILMS DURING GROWTH

During this reporting period one of the thrust areas in this research program has been the incorporation of B or Al and P or N as p- and n-type dopants, respectively, in order to produce simple discrete devices and samples for the study on the effect (if any) of dopants on the formation of stacking faults and polytypism during growth and during annealing procedures on the ion implanted samples.

In this study the dopant substances are presently incorporated directly in the primary gas stream which contains SiH_4, C_2H_4 and H_2 for the chemical vapor deposition of β-SiC. The dopant hydride gases of PH_3 and B_2H_6 contained in H_2 are employed as sources of P and B, respectively. Nitrogen in H_2 was formerly considered as a potential n-type dopant; however, no incorporation of this element in SiC at or above the $10^{17}/cm^3$ (the minimum detectable limit with the CAMECA ims-3f ion microprobe) was produced even using high flow rates of N_2. Thus NH_3 entrained in H_2 has now been ordered as a potential N source. Finally liquid trimethyaluminum (TMA) has been chosen as the Al source (in contrast to triethyaluminum (TEA) used in Japan) because (1) the methyl radical is much more stable to decomposition with the subsequent formation of unwanted C than the ethyl radical and (2) the boiling point of the TMA (293K) is lower than that of the TEA (409K). The concentration in the gas stream is altered by changing the flow rate of H_2 over the TMA. The concentrations in H_2 of all the dopant gases currently being investigated and their respective purities are given in Table I.

Table I. Concentrations and Purities of Gases Employed as Electrically Active Dopants During the CVD Growth of β-SiC.

Dopant Gases	Bottle Concentrations(Mixed Gases)	Purity
Phosphine (PH_3)	52.7 ppm (in H_2)	99.9995% (VLSI) grade
Diborane (B_2H_6)	53.0 ppm (in H_2)	99.9995% (VLSI) grade
Nitrogen (N_2)*	50.2 ppm (in H_2)	99.9995%
Trimethylaluminum [$(CH_3)_3Al$]	Liquid source at room temperature. Vapor pressure maintained constant via controlled temperature (±0.1K) bath	99.9995%

*NH_3 in H_2 has been ordered as a replacement for this gas because of the absence of detectable incorporation at 1593K.

The introduction (or lack of it) of these dopants into the β-SiC films has been analyzed quantitatively as a function of depth using the ion microprobe. As noted in the previous report, analyses of the dopant/Si ratios of ion implanted standards throughout the concentration range of the asymetric implant profile results in linear curves of the dopant/Si ratio versus concentration (e.g. see figure 6-8 in previous report) which can be used to quantitatively determine the concentration of a species in the "in-situ" doped films of β-SiC. The depth profiles for Si and P, Si and Al and Si and B are given in figures 1-12. The quantitative results from the ion microprobe analyses coupled with use of the aforementioned linear curves to give values of concentration are presented in Table II.

As implied above, the N profiles showed only background levels even at the surfaces of the films; thus no graphs of these results are presented. Similary, the 1.6 sccm PH_3 flow rate sample showed only background levels of P^+ even at the surface. However, the maximum flow rate of PH_3 in H_2 of 100 sccm produced a reasonably constant concentration profile of $\simeq 4 \times 10^{17}/cm^3$, as shown in figure 1. The reason for the higher concentrations at and near the surface of this and other profiles in this series of figures is not known at this time, but is being investigated by a variety of techniques at this writing.

The concentration of Al as well as B in the regions outside the near surface areas were found to scale in direct proportion to flow rate of the species in H_2, as shown in figures 2-10 and especially figure 12. In the case of the Al, the concentration was also directly proportional to the temperature (and, therefore, the vapor pressure) of the TMA, as noted most readily in Table II. Note that the Al profile in figure 5 has been mathematically lowered relative to the other Al plots in order to bring it onto the graph.

The ion microprobe data noted above was obtained using a 250×10^{-6}m sq scanning raster; thus, the rate of profiling was only 0.82 Å/min. However, using a 50×10^{-6}m diameter beam allowed a

100 SCCM PH3 SICP01 4/10/84

10E6
10E5
10E4
10E3
10E2
10E1
10E0

1 11 21 31 41 51

Si
P

RAW DATA

8 H 8 Mn 6 S

Figure 1. Composition profile of P^+ which has been "in-situ" doped in a β-SiC thin film using PH_3 in H_2 at a flow rate of 100 sccm.

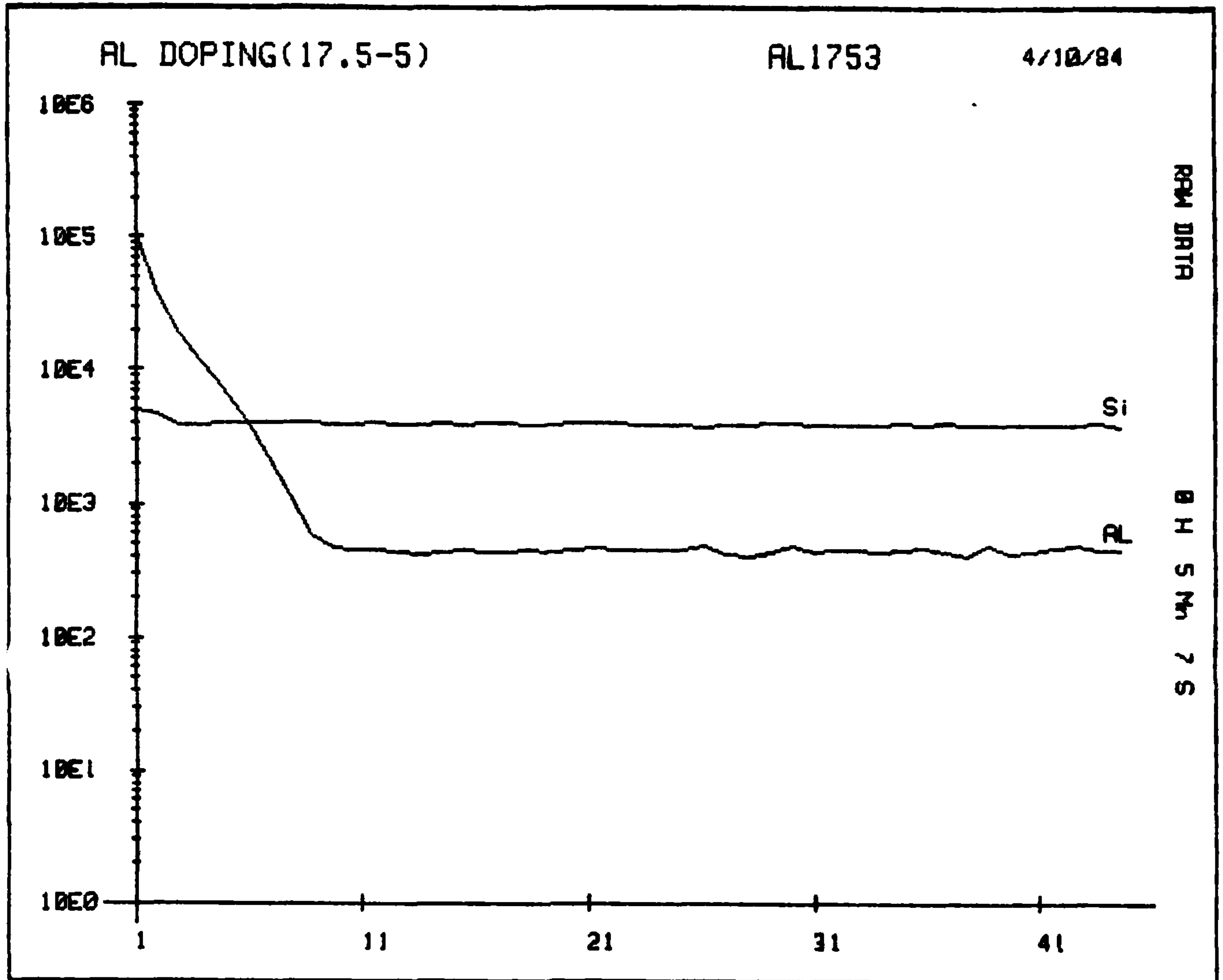

Figure 2. Composition profile of Al^+ which has been "in-situ" doped in a β-SiC thin film using TMA at a temperature of 290.5K and carried in H_2 at a flow rate of 5 sccm. The graph shows ion yield in counts vs data storage channels.

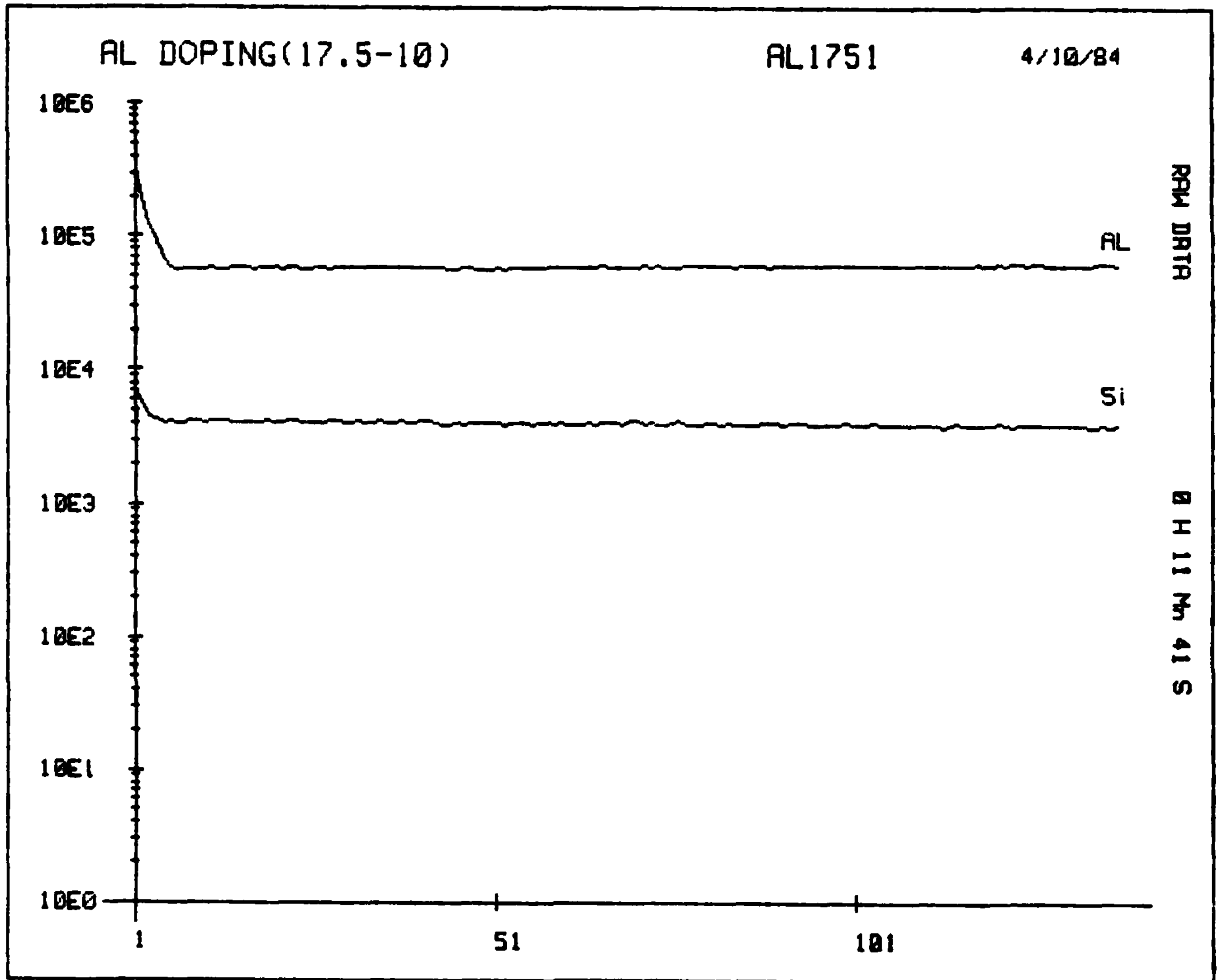

Figure 3. Composition profile of Al^+ which has been "in-situ" doped in a β-SiC thin film using TMA at a temperature of 290.5K and carried in H_2 at a flow rate of 10 sccm. The graph shows ion yield in counts vs data storage channels.

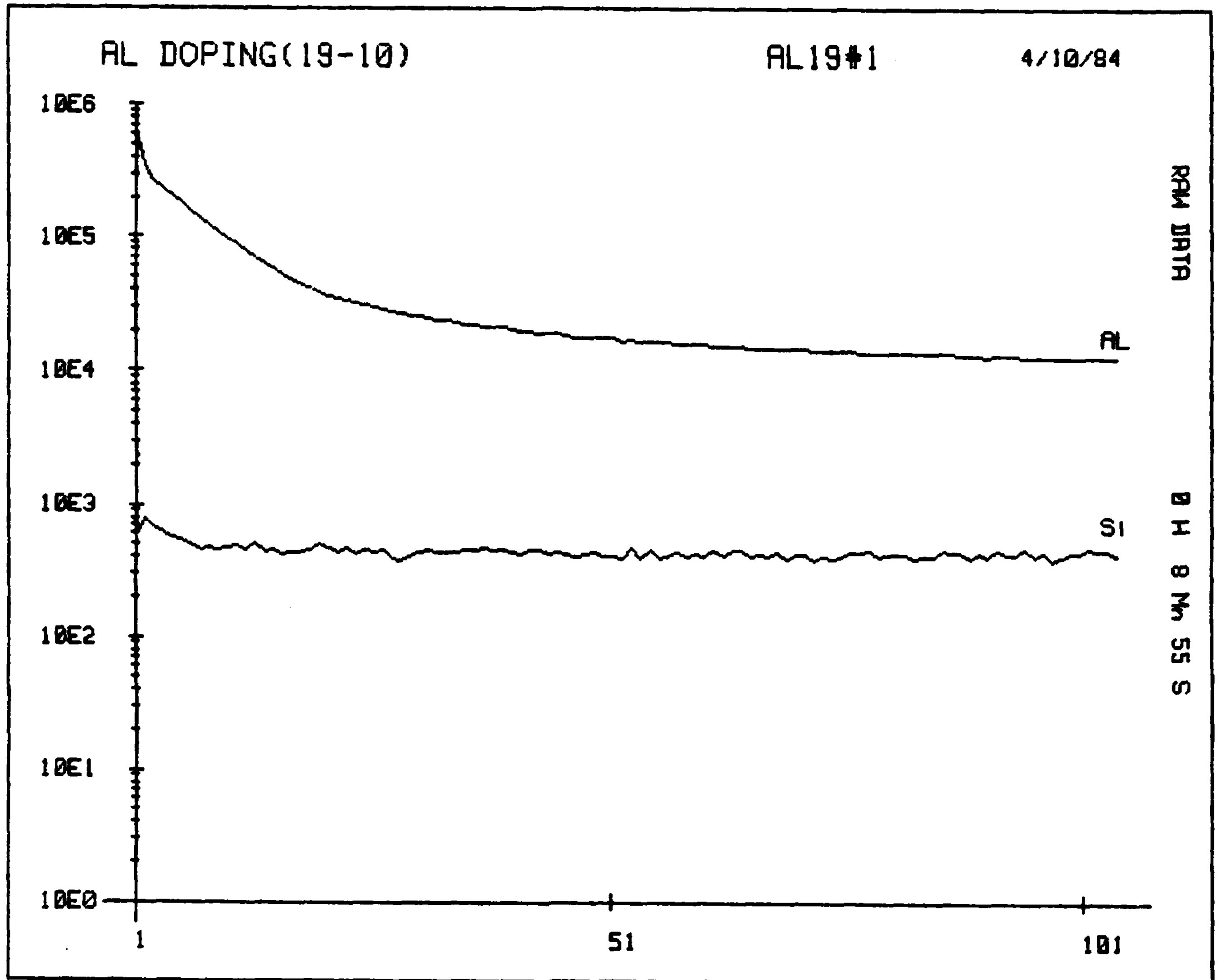

Figure 4. Composition profile of Al^+ which has been "in-situ" doped in a β-SiC thin film using TMA at a temperature of 292K and carried in H_2 at a flow rate of 10 sccm. The graph shows ion yield in counts vs data storage channels.

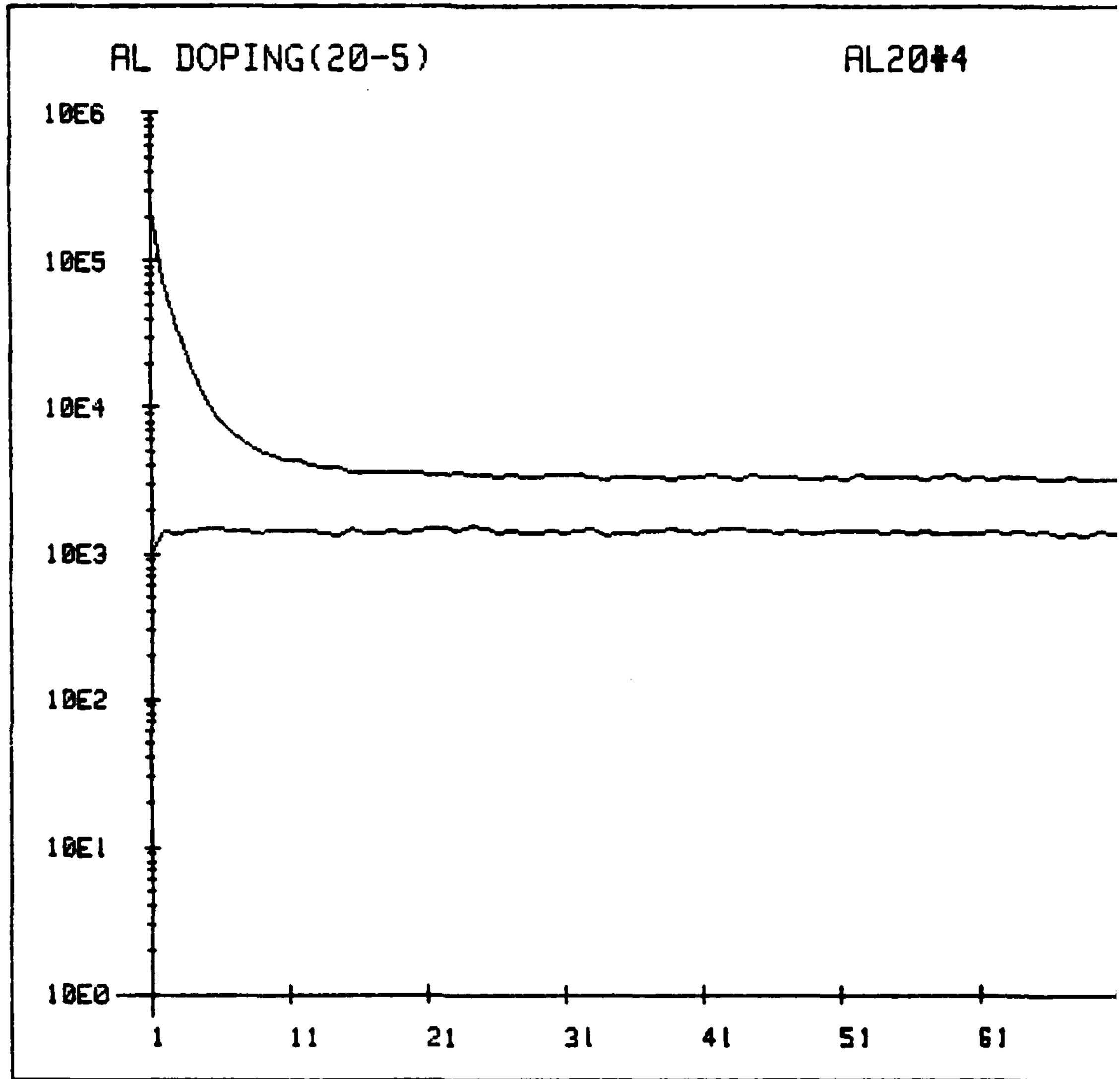

Figure 5. Composition profile of Al^+ which has been "in-sitı doped in a β-SiC thin film using TMA at a temperai of 293K and carried in H_2 at a flow rate of 5 sccr The graph shows ion yield in counts vs data storaı channels.

Figure 6. Composition Profile of B^+ which has been "in-situ" doped in a β-SiC thin film using BH_3 in H_2 at a flow rate of 5 sccm.

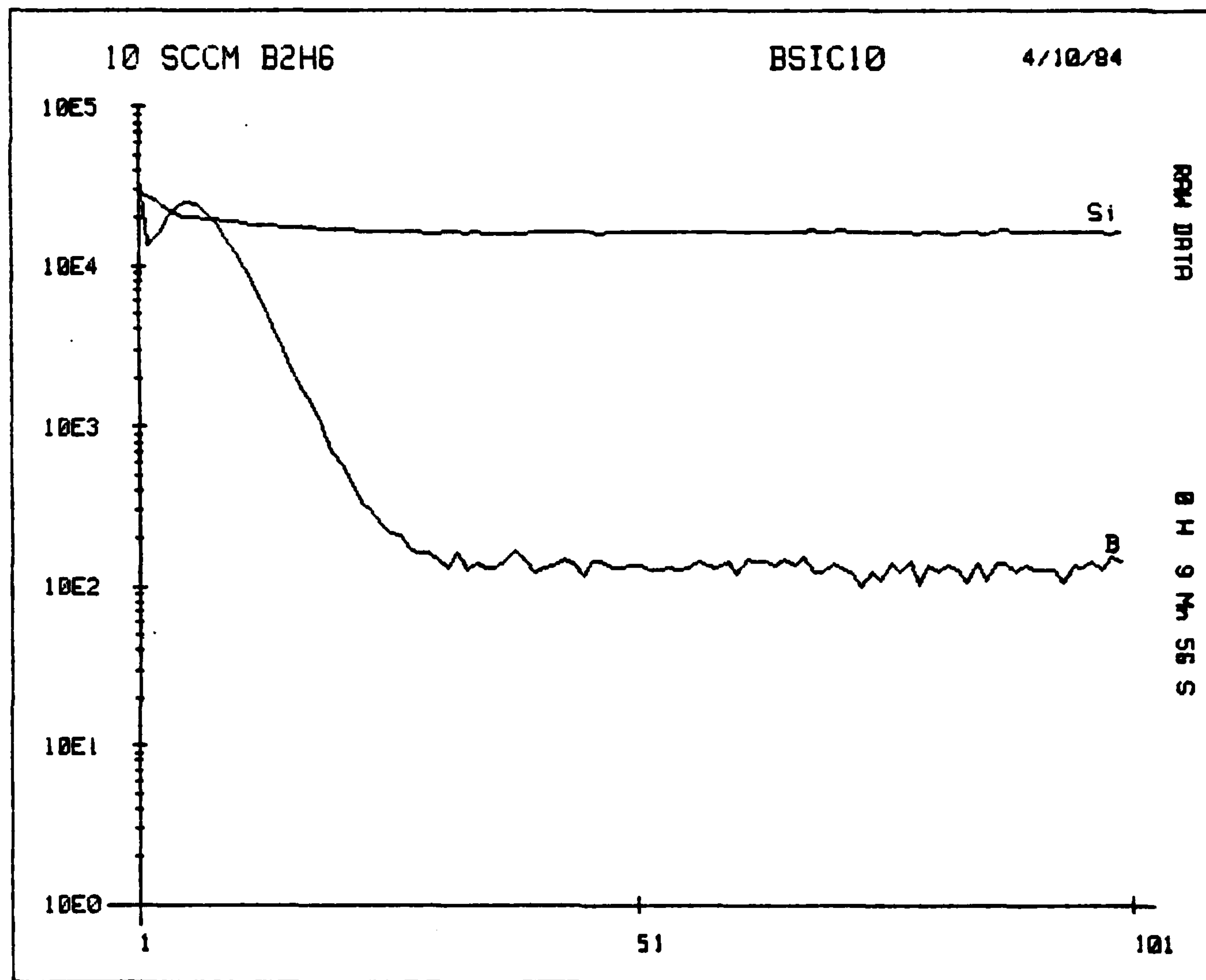

Figure 7. Composition profile of B^+ which has been "in-situ" doped in a β-SiC thin film using BH_3 and H_2 at a flow rate of 10 sccm.

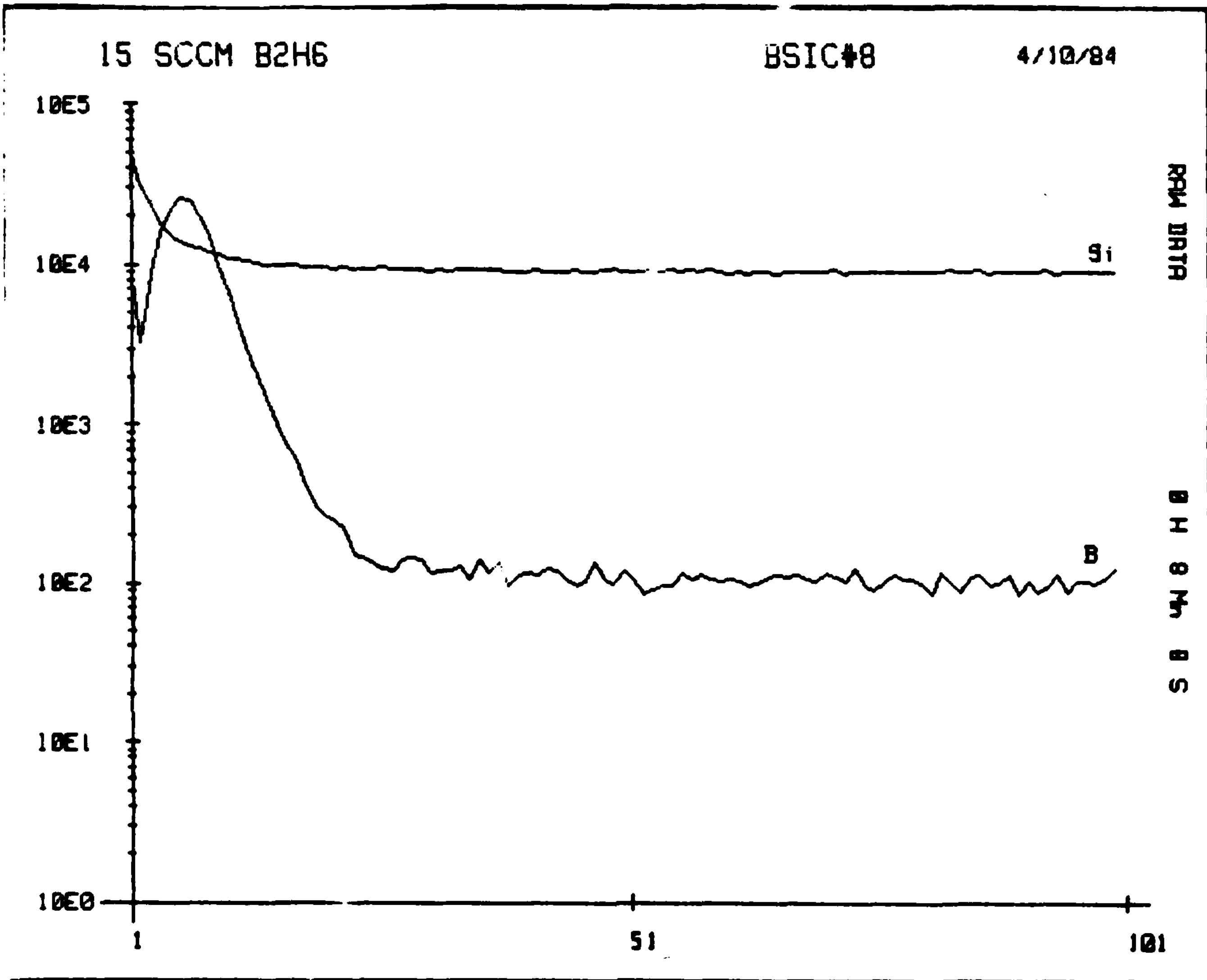

Figure 8. Composit[illegible] profile of B^+ which has been "in-situ" doped in [illegible]-SiC thin film using BH_3 and H_2 at a flow rate of [illegible]m.

Figure 9. Composition profile of B^+ which has been "in-situ" doped in a β-SiC thin film using BH_3 and H_2 at a flow rate of 20 sccm.

Figure 10. Composition profile of B^+ which has been "in-situ" doped in a β-Sic thin film using BH_3 and H_2 at a flow rate of 25 sccm.

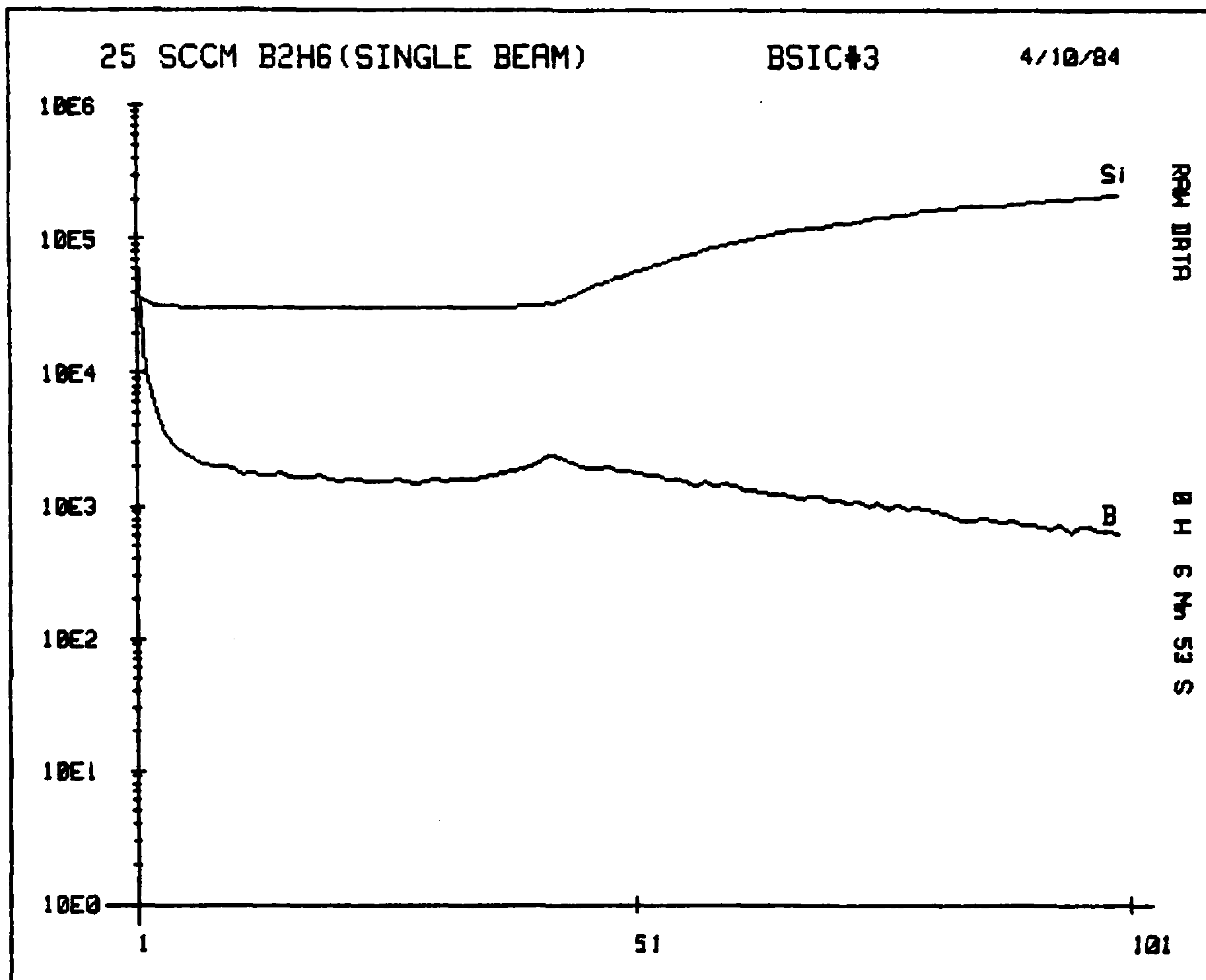

Figure 11. Composition profile of B^+ in β-SiC films. The film is the same as that described in Figure 10, except the rate of depth profiling is sufficient to penetrate completely the film such that an analysis of the B concentration in the Si substrate is also obtained. The small peak in the middle of the graph represents the β-SiC/Si interface.

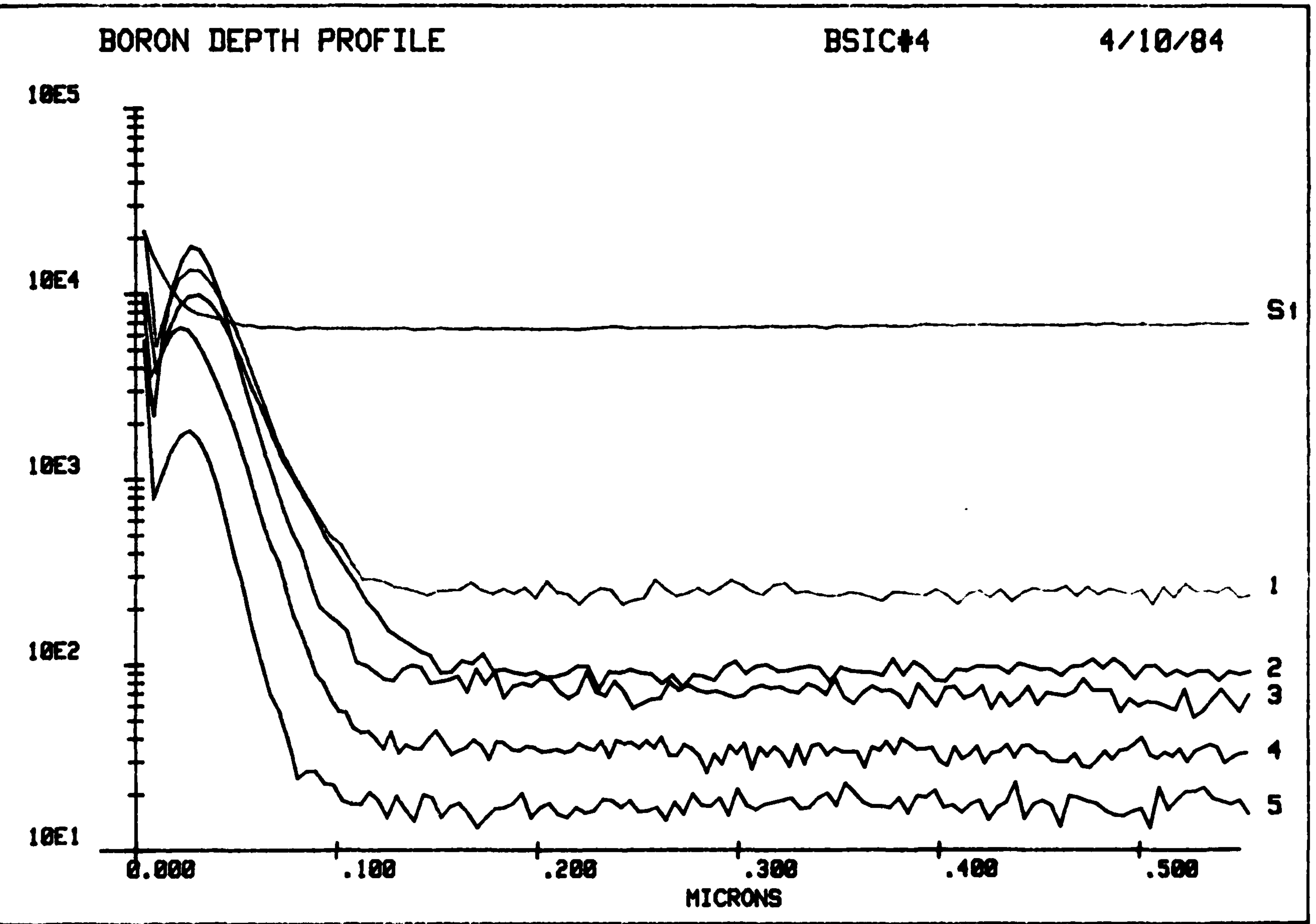

Figure 12. Compilation of figures 6-10 in terms of B^+ counts vs distance into the film for the various BH_3 in H_2 flow rates. Note that the B count beyond $\approx 0.100 \times 10^{-6}$m scales with the flow rate with curves #1-5 being the 24,20,15,10 and 5 sccm rates, respectively.

Table II. Doping Conditions, Dopant Count/Si Count Ratios and Dopant Concentrations in the As-Grown β-SiC Samples

Dopants	Dopants Gases	Flow Rates	Dopant/ Si Ratios	Dopant Concentrations (N/cm^3)
N	N_2 in H_2	20 sccm 30 sccm 100 sccm	N concentration in all samples was essentially at background levels ($\simeq 10^{17}/cm^3$) for ion microprobe detection	
P	PH_3 in H_2	1.6 sccm	2.0×10^{-5}	4.0×10^{16} (background levels)
		100 sccm	2.5×10^{-4}	4.0×10^{17}
Al	Hydrogen Flow over liquid (TMA)	17.5°C,5sccm	14.44	8.0×10^{18}
		17.5°C,10sccm	15.09	8.4×10^{18}
		19.0°C,10sccm	31.25	1.7×10^{19}
		20.0°C,5sccm	160.38	8.9×10^{19}
B	B_2H_6 in H_2	5 sccm	3×10^{-3}	5.3×10^{16}
		10	8×10^{-3}	1.3×10^{17}
		15	1.1×10^{-2}	2.8×10^{17}
		20	1.5×10^{-2}	3.4×10^{17}
		25	3.9×10^{-2}	5.3×10^{17}

much more rapid rate of profiling and complete penetration of the film and analyses of the dopant in the Si. An example of this is shown in figure 11 for B in β-SiC. The small hump in the middle of the graph is the β-SiC/Si interface. As one can see substantial diffusion of B into Si occurred during growth. Although the 10K ohm-cm resistivity Si contains B at a concentration of $\simeq 10^{12}/cm^3$, the level shown in this graph is six orders of magnitude greater than the as-received level. Furthermore, the gradient in concentration is shallow indicating that B diffusion in Si is fast at the temperature of β-SiC growth ($\simeq$1593K). The transport of B is no doubt assisted by pipe diffusion along the misfit dislocations which occur at the Si/β-SiC interface.

Profiling of the Al^+ composition through the film and into the Si also revealed a hump in Al^+ concentration at the Si/β-SiC interface of even greater magnitude than in the case of B. No such phenomonon has been observed in the P^+ profiles; however, the total amount of P^+ may be too small to contribute to this increase in composition.

Preliminary C-V measurements indicate that both the B and Al doped samples are p-type with charge carrier concentration 10^2 less than the measured dopant concentration as a result of growth at 1593K.

Work in the next period will be devoted to obtaining the incorporation of N and additional P in the β-SiC lattice, a determination of the charge carrier concentration relative to the total concentration of dopant, determination for the excess amounts of impurity at the surface and interface and the fabrication of a p-n junction.

III. ION IMPLANTATION AND ANNEALING STUDIES

The ion implantation in our β-SiC films conducted during this reporting period by the NCSU implantation facilities is shown in Table III. All starting films were undoped with n-type character and deposited on 10^4 ohm-cm p-type Si wafers. The Si triple implant samples were produced in conjunction with a P implant to determine if the regrowth of the amorphous layer produced by the former implant from a position deeper inside the sample than the latter implant could eliminate the unrecovered damage normally associated with the initial position of regrowth. In other words, dislocation loops and other damage are normally associated with the point of onset of regrowth of a heavily damaged or an amorphous layer produced by the implantation procedure. The Si was implanted to a greater depth than the maximum depth of the subsequent P implant as well as at intermediate and shallow depths by using three different implant schedules (see Table III). Cross sectional electron microscopy coupled with microdiffraction has shown this multiple implant region to be amorphous. However, damage recovery (or, at least, electrical activation of the charge carriers) has been a not unexpected problem.

According to Marsh (SiC-1973, U. of South Carolina Press, 1974 pp. 471-485), recovery of ion implanted structural damage in α-SiC is ≈95% complete after 900s at 1473K with any residual disorder being caused by nonequilibrium point and line defects. By contrast, electrical activation of implanted charge carrier species is not complete until a temperature of ≈1973K. Thus, another thrust area in this reporting period has been to ascertain if these results were also true for our β-SiC films.

Attempts to achieve electrical activation have involved the Si triple implants (also with P and Al), as well as pure Al, B and P implants noted in Table III. The initial process was rapid thermal annealing (RTA) using a Heatpulse(R) 210 with a maximum temperature capability of 1525K within 10s. Four samples were annealed in Ar at 50K intervals from 1073-1525K. The sheet resistance measurements given in Table IV provided information on the relative extent

Table III. Schedule of Beta SiC Samples and Implant Species and Conditions

Implant Species	No. of Samples	Implant Conditions Potential(keV)	Dose($1/cm^2$)	Utilization Implant Samples (No)
Si	4	80	5×10^{15}	XTEM after implantation(1)
		160	8.6×10^{15}	Annealing/resistivity study(1)
		320	1.36×10^{15}	XTEM after annealing(1)
				RBS channeling study(1)
P	8	140	4.6×10^{14}	(a) without Si triple implant
				XTEM after implantation(1)
				Annealing/resistivity study(1)
				XTEM after annealing(1)
				RBS channeling study(1)
				Extra sample(1)
				(b) with Si triple implant
				Annealing/resistivity study(1)
				XTEM after annealing(1)
				RBS channeling study(1)
Al	8	120	4.59×10^{13}	(a) without Si triple implant
				Five samples to be used in the same way as P
				(b) with Si triple implant
				Three samples to be used in the same way as P
N	3	120	1.4×10^{14}	Annealing/resistivity study(1)
				XTEM(1)
				RBS channeling(1)
B	1	200	7.6×10^{13}	Annealing/resistivity study

of activation. The data in this table shows that no activation of either Al^+ or P^+ in the Si^+ triple implant was observed. Furthermore only a slight drop in resistivity was recorded for the P^+ implant alone from 1423-1523K.

To increase the temperature further while maintaining the rapidity of heating, a special vacuum evaporation system capable of heating two samples simultaneously to temperatures in excess of 2275K was retrofitted for our annealing studies. To maintain purity, very high purity SiC-coated graphite strip heaters containing a sample cavity were employed for supplying heat to the samples. The maximum

Table IV. Effect of Rapid Thermal Annealing at Various Temperatures up to 1523K of Triple Si Ion Implants As Well As Implants of Al^+ (120 keV, 4.59 x $10^{13}/cm^2$) and P^+ (140 keV, 4.6 x $10^{14}/cm^2$) on Sheet Resistance ($ohms/cm^2$) in β-SiC Films. Annealing Time Was 10s at Each Temperature.

Anneal Temp. (K)/ Resistivity ($ohms/cm^2$)	Si^+ Triple Imp. plus Al^+	Si^+ Triple Imp. plus P^+	Al^+ in SiC	P^+ in SiC
Initial	>3000	>3000	770	1250
1073	│	│	│	│
1123	│	│	│	│
1173	│	│	│	│
1223	│	│	│	│
1273	unchanged	unchanged	unchanged	unchanged
1323	│	│	│	│
1373	│	│	│	┴
1423	│	│	│	1150
1473	│	│	│	1100
1523	┴	┴	┴	920

use temperature was limited by the 1688K melting point of the Si substrate. The results of this study for Al^+, P^+ and B^+ are given in Table V. Nitrogen implants have not yet been similarly investigated.

The results of this latter study did show a decrease in the sheet resistance for all but the Si^+ triple implant. This indicates that severe damage such as in the case of the Si^+ implants does not readily anneal out and allow activation of charge carriers as does the minor damage produced in the pure P^+, Al^+ and B^+ implants. A graph of the change in B sheet resistivity is shown in figure 13.

Table V. Effect of Thermal Annealing at Temperatures Between 1273 and 1663K of a triple Si Implant As Well As Implants of Al^+ (120 keV, 4.59 x $10^{13}/cm^2$) P^+ (140 keV, 4.6 x $10^{14}/cm^2$) and B^+ (200 keV, 7.6 x $10^{13})/cm^2$) on Sheet Resistance ($ohms/cm^2$) in β-SiC Films. Annealing Time Was 3.0 x 10^2s at Each Temperature.

Anneal Temp. (K) Resistivity($ohms/cm^2$)	Si Triple Imp. plus Al^+	Al^+ in SiC	P^+ in SiC	B^+ in SiC
Initial	>3000	770	1150	1050
1273	│	│	1150	905
1473	unchanged	unchanged	620	820
1573	│	┴	575	790
1663	┴	730	450	-

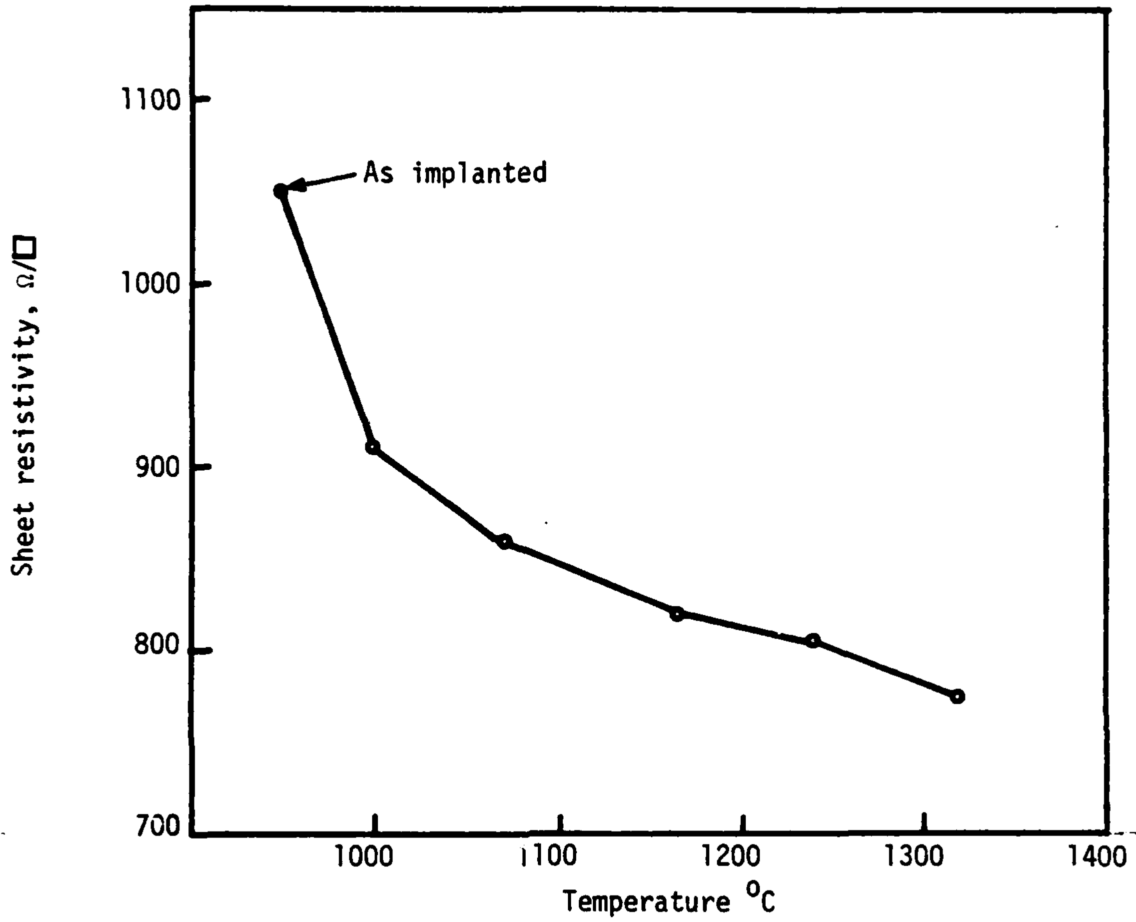

Figure 13. Variation in sheet resistivity with annealing temperature of β-SiC, implanted with boron at a dose level of 7.6×10^{13} cm^{-2} at 200 kev. Annealing time at each temperature was 5 min.

Because the drop in resistivity was very small, it is be
lieved that much higher annealing temperatures are now necess
Thus, this work in implanted β-SiC confirms that found by Mar
At present we are attempting to remove the Si substrate, appl
a substitute substrate and anneal at much higher temperatures

To conduct this Si substrate replacement task, the thin film/substrate combination is placed SiC face down onto a gla slide and bonded with a high thermal conductivity epoxy coati which is subsequently cured. The samples are then immersed i 1:1 HF:HNO_3 mixture which etches the Si from the β-SiC film.

The current candidates of choice for the new substrates r-f sputtered onto the β-SiC film are Al_2O_3 and W, both of wh have similar thermal expansion coefficients (especially W) to β-SiC as well as a high melting point. The requisite targets have just been received and research begun (see section V). Thus another task during the next reporting period will be to develop the full technique for acquiring the new coated subst on the β-SiC film.

IV. OXIDATION STUDIES

Work throughout this reporting period has also involved the establishment of a complete system for the oxidation of the SiC films. Although progress in this work was hampered by vendor delivery of glassware, changes in design to accommodate the high temperatures and electrical problems with the furnace power supply, the unit is now operational and initial runs have been completed. An operational schematic of the complete system is shown in figure 14; a description of the flow path is given below.

The system, as presently configured, utilizes high purity O_2 or Ar introduced into a tube furnace containing the β-SiC films. The O_2 can be either dry or saturated with H_2O vapor via a heated (370K) three liter flask containing deionized water. The latter process produces the more rapid oxidation. The stainless steel tubing carrying the wet O_2 to-and-from the furnace is heated (373K) to prevent condensation. A vacuum pump is also attached to the system to allow the fused silica furnace tube and associated tubing to be evacuated and backfilled with 99.9995 Ar in order to mitigate the possibility of nitrogen doping. The baffles and the boat containing the samples are pulled in-and-out with a quartz pull rod and can be placed on a quartz boat holder for subsequent handling. The exhaust bubbler contains a low vapor pressure Si-based diffusion pump oil. The dry "bubbler" is used to prevent any backstreaming of this oil, in the event of a pressure drop below atmospheric.

In the current oxidation scenario, the samples are placed in the furnace, which is maintained at 773K and the end cap replaced. After a vacuum is achieved, the tube is backfilled with Ar to atmospheric pressure, the exhaust valve opened to the exhaust bubbler and the furnace heated to 1473-1523K. Wet or dry O_2 is then introduced. After oxidation, the samples are annealed in Ar to allow any oxygen remaining in the grown oxide to react, subsequently cooled and the samples removed from the furnace.

Initial oxidation studies have produced excellent electrical isolation of the SiC films. The present SiO_2 layers are thin

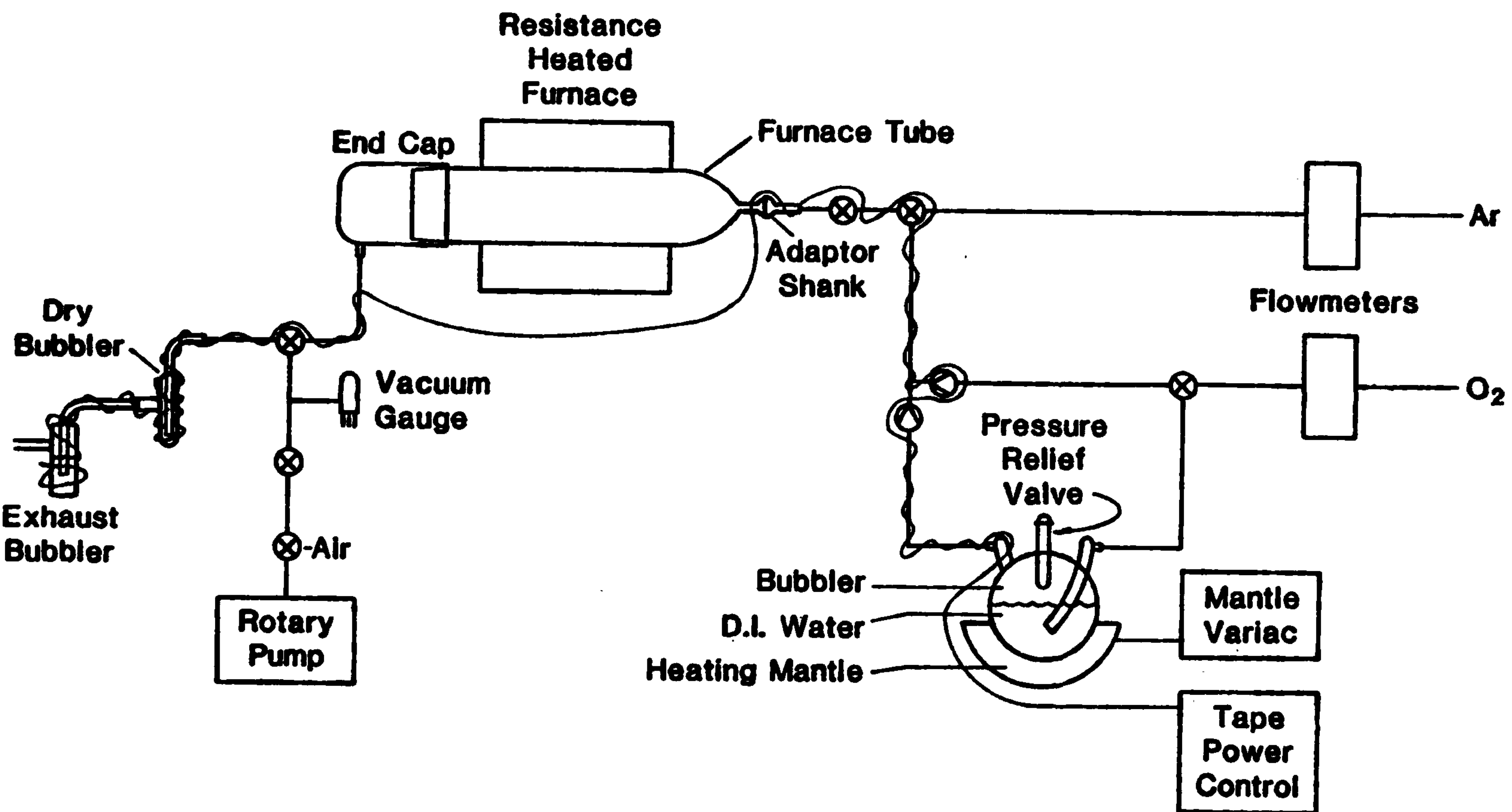

Figure 14. Schematic of the thermal oxidation system used to oxidize the β-SiC thin films.

(≈60 nm). Future research will concentrate on making slightly thicker layers and, more importantly, on the effect of the oxidation procedure on the removal of implanted or grown-in dopants near the oxide/SiC interface and on the development of accurate measurements of oxide thickness.

V. PLASMA ETCHING AND RF SPUTTERING RESEARCH

Plasma etching of the β-SiC films has also been conducted during this reporting period using a recently retrofitted MRC four target unit operating at 100 watts. At the best possible tuning (≈12% reflected power), a SiC etch rate of 33 Å/min was achieved. Some time was also spent investigating the possibility of enhancing this rate by adapting the system to perform reactive ion etching. However, because of the effects of the corrosive by-products of reactive ion etching on the existing equipment, the lack of adequate exhaust facilities in this particular laboratory and the absence of any need to quickly remove large amounts of material, the employment of this process has been put aside at this writing.

As noted in Section III, r-f sputtering of Al_2O_3 and W onto the backside of the β-SiC film will be tried as a high melting point and rigid substitute for the Si substrate so that implant annealing studies can be conducted. To this end, both materials have been sputter deposited at a power level of 200 watts. Sputtering rates of 8.3-10.0 nm/min for W and 7.0-7.5 nm/min for Al_2O_3 have so far been achieved.

Progress on this study was slowed because the heater on the diffusion pump burned into. Because of back orders, receipt of a new part required seven weeks. The system is also currently being changed from a one target to a three target system in order to conduct these studies more efficiently.

VI. DEVICE FABRICATION AND ELECTRICAL CHARACTERIZATION

In order to be able to make I-V and Hall measurements and to electrically characterize the single devices described below, it has been necessary to develop proper ohmic contacts for n- and p-type β-SiC. Although In is a reasonably good ohmic material, its temperature range of usefulness above 273K is limited. Thus, it was decided from the outset to develop contacts which could be used at much higher temperatures. Our initial efforts have resulted in the development, fabrication and use of a 3% Ta/97% Au alloy for n-type SiC and alloys of 2.3% Ta/7.3% Al/90.4% Au as well as 11% Si/89% Al for p-type SiC. The melting point of the last alloy is ≃823K; thus, it can only be used at moderate temperatures. During the next reporting period, additional work on other contact materials will be conducted.

Fabrication of Schottky diodes at the end of the previous reporting period using undoped β-SiC films and ohmic and retifying contact materials of 3% Ta/97% Au and Au, respectively, produced disappointing results. I-V measurements revealed a low breakdown voltage and high leakage currents. Differential C-V measurements using H_g contacts indicated very high carrier concentrations at the surface. This type of problem has also been reported for GaAs grown from the vapor phase.(M. J. Cardwell and R. F. Peart, Electron. Lett. 9, 88 (1973) and D. L. Lile and L. L. Taylor, Ibid. 14-15, 457 (1978)).

Improvements in the growth procedures and the utilization of oxidation facilities wherein the near-surface region can be removed by HF etching of the oxide have allowed considerable improvements in device performance. Figure 15 shows much improved I-V characteristics for a β-SiC film having a charge carrier concentration of $\simeq 9 \times 10^{15}/cm^3$. In this case In and Au were used as the ohmic and rectifying contacts, respectively. The area of the junction was $1.6 \times 10^{-7} m^2$. The sample had also been twice oxidized at 1423K for $7.2 \times 10^3 s$ and etched in buffered HF prior to device fabrication. Although notable leakage current exists, breakdown did not occur up to a maximum applied voltage of -50 V. Thus, in these latter samples,

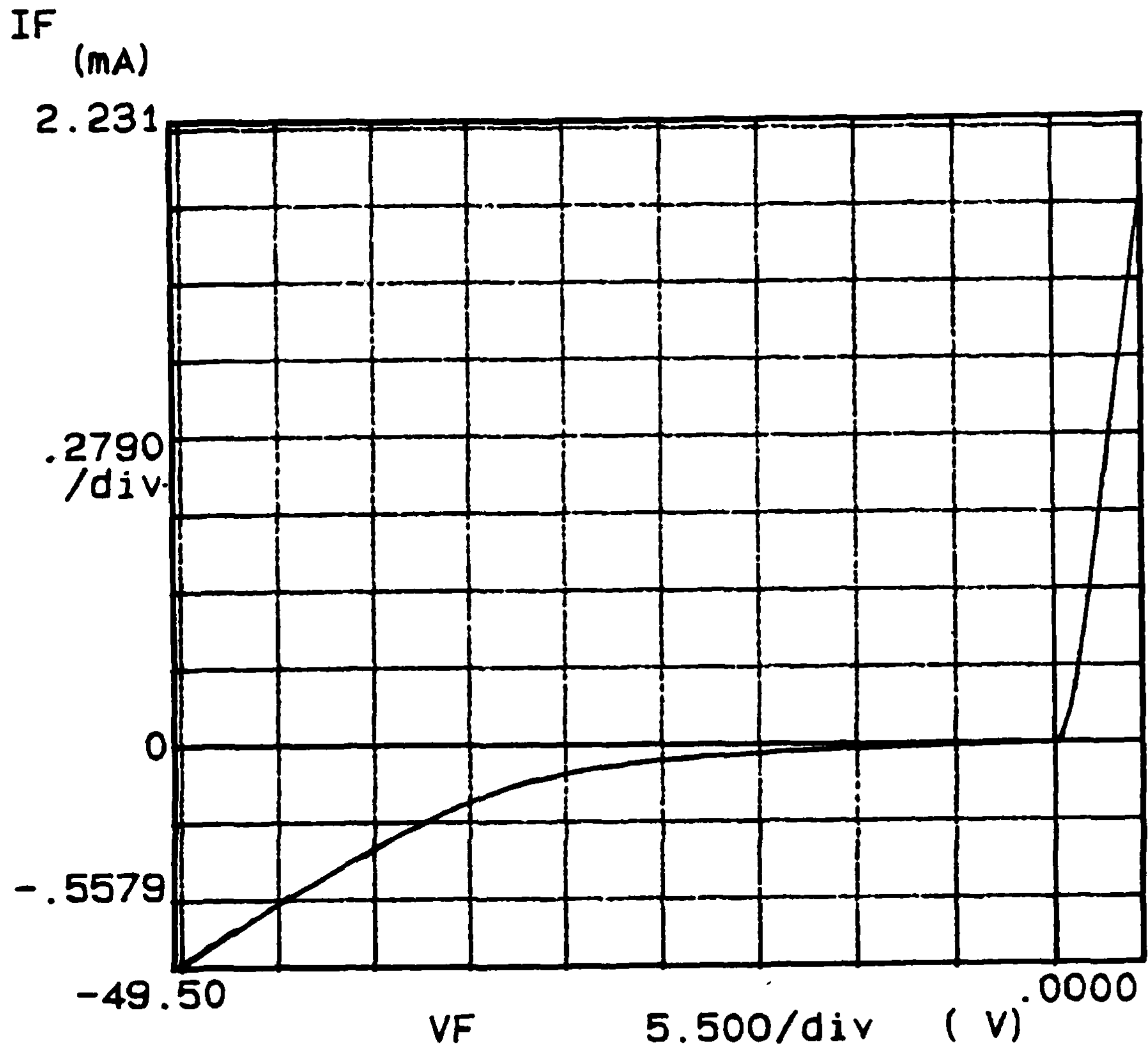

Figure 15. I-V Characteristics of 1.6×10^{-3} cm^2 planar Schottky diode composed of Au rectifying contact and In ohmic contact. The SiC sample was twice oxidized and etched in buffered HF prior to the evaporation of the contact materials.

the primary source of leakage current may be bulk defects such as stacking faults and dislocations.

The research group has also been preparing to produce MOSFET structures. A flow schedule has been derived for this work as shown in Table V. Initial masks have been computer generated using the new CALMA mask making facility (line width maximum = 0.5 μm). Modifications to other systems to be employed in this process to handle the 1.0 cm wafers are now underway.

Table V. Flow Schedule for Fabrication of a β-SiC MOSFET (for n-channel device)

1) Oxidize film (1000 Å)
2) Evaporate 1-2 μm Al (as an implant barrier)
3) Apply photoresist and bake
4) Employ 1st mask - align - expose (uv) - develop
5) HF etch
6) Phosphorous implant
7) Remove photoresist, Al and SiO_2
8) a) Mount sample on glass-slide Si side up
   b) Etch off Si
   c) Sputter on Al_2O_3 (~2 μm) and W (~10 μm) or SiC (~10 μm)
9) Remove sample
10) Anneal
11) Reoxidize 1000 Å (gate oxide)
12) Reapply sample to Si substrate
13) Continue with photo steps for other maskings
14) Metallization
15) Contacts

DISTRIBUTION LIST - ANNUAL LETTER REPORT

CONTRACT N00014-82-K-0182

Address	No. of Copies
Dr. Max Yoder Office of Naval Research Electronics Program - Code 427 800 North Quincy Street Arlington, VA 22217	2
Ms. Nancy S. McHan ONR Resident Representative Georgia Institute of Technology 214 O'Keefe Building Atlanta, GA 30332	2
Director, Naval Research Laboratory ATTN: Code 2627 Washington, DC 20375	7
Defense Technical Information Center Bldg. 5 Cameron Station Alexandria, Virginia 22314	14
ONR Branch Office 536 South Clark Street Room 286 Chicago, IL 60605	2
Dr. J. Anthony Powell NASA Lewis 2100 Brookpark Rd. Cleveland, OH 44135	1
Dr. Ray Kaplan Code 6834 Department of the Navy Naval Research Laboratory Washington, DC 20375	1

END

FILMED

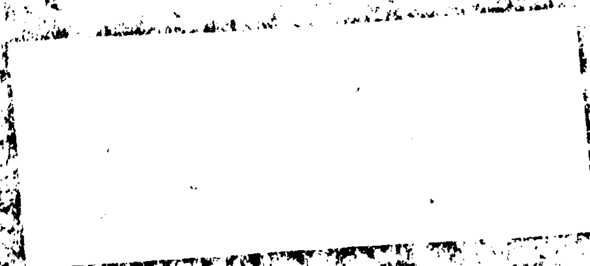

DTIC